

A reduced-complexity model for river delta formation – Part 2

M. Liang et al.

This discussion paper is/has been under review for the journal Earth Surface Dynamics (ESurfD). Please refer to the corresponding final paper in ESurf if available.

A reduced-complexity model for river delta formation – Part 2: Validation of the flow routing scheme

M. Liang^{1,2}, N. Geleynse^{2,*}, D. A. Edmonds³, and P. Passalacqua¹

¹Department of Civil, Architectural and Environmental Engineering and Center for Research in Water Resources, The University of Texas at Austin, Austin, Texas, USA

²Department of Geological Sciences, The University of Texas at Austin, Austin, Texas, USA

³Department of Geological Sciences, Indiana University, Bloomington, Indiana, USA

*now at: ARCADIS, Water and Environment Division, Amsterdam, the Netherlands

Received: 25 June 2014 – Accepted: 7 July 2014 – Published: 28 July 2014

Correspondence to: M. Liang (manliang@utexas.edu)

Published by Copernicus Publications on behalf of the European Geosciences Union.

Title Page

Abstract

Introduction

Conclusions

References

Tables

Figures



Back

Close

Full Screen / Esc

Printer-friendly Version

Interactive Discussion



process is given in the discussion section based on the results of test 4a. Therefore we run the code over a large number of iteration steps, typically 500 to 1000, which is more than what is needed to achieve convergence.

The key step is calculating the probabilities for routing water parcels, based on rules abstracting the governing physics – hence the name “weighed-random-walk”. As the detailed procedure is explained in Part 1, here we only revisit the main idea. The likelihood of a neighbor cell to receive a water parcel is determined by a combination of local quantities including water surface gradient, the direction of flow inertia, and flow depth at the cell. In other words, if a cell is more aligned with the local “downstream” direction and has greater water depth, then its probability of receiving water parcels from nearby cells is higher.

The steps for calculating the routing probability field are:

2.1 Step 1: define a routing direction at each cell

The routing direction (F) is essentially an estimate of local downstream direction for the purpose of directing the water flux. In our model, it is a combination of the estimated local water surface gradient and direction of flow inertia:

$$F^* = \gamma F_{\text{sfc}} + (1 - \gamma) F_{\text{int}}, \quad (1)$$

$$F = \frac{F^*}{|F^*|}, \quad (2)$$

where $F_{\text{int}} = \frac{\mathbf{q}}{|\mathbf{q}|}$ is a unit vector indicating inertia, and $F_{\text{sfc}} = \frac{\nabla H}{|\nabla H|}$ is a unit vector indicating surface gradient. Both \mathbf{q} and ∇H take value from the latest iteration step. γ is a dimensionless coefficient, which is set to 0.05 in our runs if not indicated otherwise (Liang et al., 2014).

A reduced-complexity model for river delta formation – Part 2

M. Liang et al.

Title Page

Abstract

Introduction

Conclusions

References

Tables

Figures

◀

▶

◀

▶

Back

Close

Full Screen / Esc

Printer-friendly Version

Interactive Discussion



2.2 Step 2: calculate relative routing weights for the neighbors at each cell

With the routing direction F specified, the relative routing weights (w_i) for neighbors around each cell (8 neighbors in the case of square lattice setup) are determined as follows:

$$w_i = \frac{h_i \max(0, F \cdot d_i)}{\Delta_i}, \quad i = 1, \dots, 8. \quad (3)$$

The cellular direction vector, d_i , is a unit vector pointing to neighbor i from the given cell; Δ_i is the cellular distance (taking a value of 1 for cells in main compass directions and a value of $\sqrt{2}$ for corner cells), and h_i is water depth and neighbor i .

2.3 Step 3: calculate routing probabilities (p_i)

The weights above are then processed according to the wet-dry status of cells. The model considers cells with flow depth greater than a threshold value (typically 1–5% of the characteristic flow depth of the system) as “wet” cells, and the opposite as “dry” cells. The weights for dry cells are then converted to the value of 0. The routing probabilities (p_i) are calculated as:

$$p_i = \frac{w_i}{\sum_{nb=1}^8 w_{nb}}, \quad i = 1, \dots, 8, \quad (4)$$

where nb is the numbering of neighbors around a given cell (1 to 8 for a 3-by-3 square grid). With the routing probabilities calculated, water parcels are released one by one from the upstream inlet cells and each of them does a “directed-random-walk” based on the probability field. The cumulative movements of parcels are summed in terms of vectors at each cell to obtain an estimation of flow unit discharge.

The calculation of the water surface profile is based on a 1-D scheme along the water parcel paths, rather than the solution of a system of partial differential equations. The

A reduced-complexity model for river delta formation – Part 2

M. Liang et al.

Title Page

Abstract

Introduction

Conclusions

References

Tables

Figures

◀

▶

◀

▶

Back

Close

Full Screen / Esc

Printer-friendly Version

Interactive Discussion



basic assumption is that the water surface profile along a streamline can be approximated by a 1-D equation. In the morphodynamic results in Part 1, this 1-D equation takes the simplest form that water surface slope on the delta equals a constant value – the “reference slope”. In this hydrodynamic validation work, we formulate the 1-D equation such that (i) it satisfies the backwater equation if the local Froude number is low ($Fr^2 \leq 0.5$) and (ii) the water surface slope (S) is equal to the friction slope (S_f) if the Froude number is high ($Fr^2 > 0.5$):

$$\frac{\partial h}{\partial l} = \frac{S - S_f}{1 - Fr^2}, \text{ if } Fr^2 \leq 0.5, \quad (5)$$

$$\frac{\partial H}{\partial l} = S_f, \text{ if } Fr^2 > 0.5, \quad (6)$$

where C_f is the coefficient of friction, $S_f = C_f Fr^2 = C_f \frac{U^2}{gh}$ is the friction slope and l is the distance along an arbitrary flow streamline.

This calculation is done along each water parcel path via a finite difference scheme. An average value is taken for cells belonging to multiple paths. The obtained surface profile is then smoothed with numerical diffusion to remove bumps and ditches caused by the gaps between different 1-D paths. In addition, an under-relaxation is applied for numerical stability between iterations (see Part 1 for details).

3 Validation cases

The validation cases are designed to illuminate two important aspects in the RCM. First, we target the “reduced-complexity” features in our flow routing model, i.e. the rules and parameterizations that represent governing physics; second we want to capture critical hydrodynamic processes affecting the overall delta morphology. The hydrodynamics of river deltas involve a hierarchy of processes occurring at a wide range of scales, from flow structures behind individual ripples on the bed to channel avulsions

A reduced-complexity model for river delta formation – Part 2

M. Liang et al.

Title Page	
Abstract	Introduction
Conclusions	References
Tables	Figures
◀	▶
◀	▶
Back	Close
Full Screen / Esc	
Printer-friendly Version	
Interactive Discussion	



that change the distribution of water flux across the entire delta surface. We focus on hydrodynamic processes at the channel scale, which are essential to creating, maintaining and modifying a distributary channel network. The proposed validation tests are: (1) backwater profile in a straight channel, (2) flow around a mouth-bar, (3) partitioning of flow at a single bifurcation, (4) partitioning of flow in a distributary channel network with submerged islands. A description of each test case is given below.

3.1 Test 1: backwater profile in a straight channel

River deltas have subtle topography and water surface gradients and flow is typically subcritical. Nevertheless, the gradient in the surface profile is essential to water motion in deltaic environments (Edmonds and Slingerland, 2008). As mentioned in the previous section, FlowRCM estimates the water surface based on the assumption of a 1-D surface profile along flow streamlines. As the movement of water parcels on the grid is in both x and y direction, the calculations along these paths involve projecting each step a parcel makes to the estimated flow streamline. Thus, in the first test we use a straight channel of constant width with no variation in cross-stream direction, whose surface can be described by the 1-D backwater equation. The model performance is compared to the theoretical backwater profile.

The domain is 2000 m wide and 15 000 m long with a rectangular cross-section (Fig. 2). The bed has a constant slope $S = 10^{-3}$ and a constant friction coefficient $C_f = 0.01$. A constant discharge of $2 \times 10^4 \text{ m}^3 \text{ s}^{-1}$ is fed into the upstream inlet. The downstream outlet has a fixed water surface elevation as boundary condition. The discharge is chosen so that the flow remains subcritical in normal flow conditions. By varying the downstream water surface elevation relative to that of the normal flow, different backwater profiles can be achieved, such as M1, M2 and normal flow (Chow, 1959) (Fig. 2). As the flow does not have cross-stream variation, the surface profile can be resolved using the 1-D backwater equation (Eq. 5).

A reduced-complexity model for river delta formation – Part 2

M. Liang et al.

Title Page

Abstract

Introduction

Conclusions

References

Tables

Figures

◀

▶

◀

▶

Back

Close

Full Screen / Esc

Printer-friendly Version

Interactive Discussion



For the FlowRCM calculation, we use a grid of 20×150 cells, with cell size of 100 m. The water surface elevation calculated from FlowRCM is averaged in the cross-stream direction and compared to the numerical solution of Eq. (5).

3.2 Test 2: flow around a mouth bar

The formation of channel bifurcations is essential to the formation of the distributary channel network on river deltas (Edmonds and Slingerland, 2007; Kleinhans et al., 2013). Therefore the ability of a numerical model to represent the bifurcation process is of great importance. As shown by the work of Edmonds and Slingerland (2007), mouth bar development is critical to bifurcation. Particularly, one key feature in this process is the transition from flow acceleration to deceleration over the top of the mouth bar as the bar height grows and the bar top approaches the water surface (Fig. 3). Here we design a similar test with variable bar heights. The mouth bar topography is represented by a Gaussian-shaped bump in a straight channel. The bump does not deform and its height is varied from 10 to 99 % of the normal flow depth.

The domain is a straight channel section, 100 m wide and 200 m long with rectangular cross-section. The bed has a constant slope $S = 2.5 \times 10^{-3}$ and a constant friction coefficient $C_f = 0.1$. A constant water discharge of $50 \text{ m}^3 \text{ s}^{-1}$ is fed into the upstream inlet. The downstream outlet has a fixed water surface elevation as downstream boundary condition. The Gaussian-shaped bump has a diameter equal to approximately one third of the channel width. The side walls of the channel have a no flow boundary condition. FlowRCM uses a 40×80 grid with cell size of 25 m. Both FlowRCM and Delft3D are setup in exactly the same manner.

We compare the outputs from FlowRCM and Delft3D in terms of water surface elevation and flow velocity, focusing on: (i) the location of “hot spots” of high and low velocity (ii) the deformation of the water surface in proximity of the bump, and (iii) the transition of flow velocity right over the top of the bump as the bump height increases from 10 to 99 % of the normal flow depth.

A reduced-complexity model for river delta formation – Part 2

M. Liang et al.

Title Page

Abstract

Introduction

Conclusions

References

Tables

Figures

◀

▶

◀

▶

Back

Close

Full Screen / Esc

Printer-friendly Version

Interactive Discussion



3.3 Test 3: flow through a single bifurcation

Bifurcations control the partitioning of water and sediment in the deltaic system and affect the stability of the whole network (Edmonds and Slingerland, 2008; Edmonds et al., 2010; Kleinhans et al., 2008, 2013). Our goal here is to use simple and idealized bifurcation topography to test the response of FlowRCM to bifurcation asymmetry, e.g. changes in width and/or depth ratio of the two downstream branches.

There are three groups of tests, referred to as group A, B and C. In all groups the main channel splits into two branches that open at an angle of 60° , and both branches enter a basin with constant depth (Fig. 4). Channel banks are no-flow boundaries so that the water flux stays in the channel and there is no flooding onto the bank. For all tests FlowRCM uses a 100 by 100 grid. Group A and B have smaller domain size which is 2500 m by 2500 m with 25 m grid size, and total input discharge of $3000 \text{ m}^3 \text{ s}^{-1}$. Group C have larger domain size of 5000 m by 5000 m with 50 m grid size, and total input discharge of $5000 \text{ m}^3 \text{ s}^{-1}$. Group A explores the effect of asymmetry in depth alone, keeping the two branches at same width; group B explores the effect of asymmetry in width alone, keeping the two branches at same depth; group C explores the effect of asymmetry in cross-sectional area, by keeping the summation of the cross-sectional areas constant and all channels at the same width-to-depth ratio. Detailed channel geometries are shown in Fig. 4.

The output of FlowRCM is compared to Delft3D in terms of: (i) the spatial pattern of flow velocity and water surface elevation and (ii) the ratio of fluxes between the two branches.

3.4 Test 4: flow through a distributary channel network

In the last test, we evaluate the performance of FlowRCM at the scale of a complete deltaic distributary channel network. Specifically, we are interested in assessing whether the “inaccuracy” of the flow field at finer scales accumulates as the flow propagates through the whole channel network. The topography setups used to run

ESURFD

2, 871–910, 2014

A reduced-complexity model for river delta formation – Part 2

M. Liang et al.

Title Page

Abstract

Introduction

Conclusions

References

Tables

Figures

◀

▶

◀

▶

Back

Close

Full Screen / Esc

Printer-friendly Version

Interactive Discussion



FlowRCM and Delft3D are: the synthetic topography of a natural river delta (Test 4a) and a DeltaRCM simulated topography (Test 4b).

3.4.1 Test 4a: synthetic Wax Lake Delta (WLD) topography

Wax Lake Delta (WLD) is a modern river-dominated delta in the coast of Louisiana, part of the Mississippi River Delta system (Roberts et al., 1980; Wellner et al., 2005; Shaw et al., 2013). We constructed a synthetic bathymetry (Fig. 5) from satellite images and bathymetry measurements along 9 transects (USACE survey, 1999). We used an image processing software (Adobe Photoshop CS6) to integrate the planview of islands and channels from the satellite imagery and obtain a smooth profile between neighboring transects. FlowRCM and Delft3D are given the same initial and boundary conditions: an upstream inlet channel discharge of $2490 \text{ m}^3 \text{ s}^{-1}$ and a water surface elevation at the downstream boundary of 0 m. The friction coefficient is set to 0.01. Both FlowRCM and Delft3D use a 200 by 200 grid with cell size of 60 m.

3.4.2 Test 4b: bed topography generated by the DeltaRCM

For this test, delta topography is taken from a snapshot of the mixed grain size delta simulated by DeltaRCM. The delta is composed of 70 % fine grain and 30 % coarse grain, and has a very well-defined distributary channel network (Liang et al., 2014) (Fig. 5). The rectangular domain is 6 km wide and 3 km long. The inlet channel has a discharge of $1250 \text{ m}^3 \text{ s}^{-1}$, and the delta is formed in a basin with a constant depth of 5 m. Both FlowRCM and Delft3D use a 60 by 120 grid with cell size of 50 m.

The Delft3D simulations in both Test 3 and Test 4 were done in depth-averaged mode. The time step is 30 s and we use a constant horizontal eddy viscosity ($1 \text{ m}^2 \text{ s}^{-1}$) and a constant Chezy coefficient ($65 \text{ m}^{1/2} \text{ s}^{-1}$).

ESURFD

2, 871–910, 2014

A reduced-complexity model for river delta formation – Part 2

M. Liang et al.

Title Page

Abstract

Introduction

Conclusions

References

Tables

Figures

◀

▶

◀

▶

Back

Close

Full Screen / Esc

Printer-friendly Version

Interactive Discussion



4.3 Test 3 results: flow through a single bifurcation

To evaluate the effects of channel geometry asymmetry on flow partitioning between the bifurcations, we calculate two values from each test result for both FlowRCM and Delft3D: the asymmetry of discharge ψ_Q and the asymmetry of cross-sectional area

$$\psi_Q = \frac{|Q_L - Q_R|}{Q_L + Q_R}, \quad (7)$$

$$\psi_A = \frac{|A_L - A_R|}{A_L + A_R}, \quad (8)$$

where Q_L and Q_R are the water discharge in the left and right branch respectively; A_L and A_R are the cross-sectional area (calculated with bed elevation and resolved water surface elevation) of the left and right branch respectively.

The asymmetry values defined in Eqs. (7) and (8) are plotted in Fig. 9. FlowRCM captures the same trend of flow discharge partitioning predicted by Delft3D: the amount of water flux into the two branches is proportional to the cross-sectional area of the branches. This means that despite the variation in the ratio of depth and/or width, the flow tends to have the same mean velocity in both branches. Also, both FlowRCM and Delft3D predict a water surface gradient in the shallower branch that is significantly higher than the one in the deeper branch, consistent with field observations by Edmonds and Slingerland (2008). In quantitative terms, FlowRCM tends to over-predict surface elevation by up to 12 centimeters, and predicts a discharge asymmetry within 7% difference compared to Delft3D (Table. 1). An example of flow field and water surface elevation (test C3) is plotted in Fig. 10. Also, within each test group both FlowRCM and Delft3D predict the same behavior of upstream water surface elevation in response to the discharge asymmetry: in group A and C the upstream water surface elevation decreases as discharge asymmetry increases; in group B the upstream water surface elevation increases as discharge asymmetry increases.

A reduced-complexity model for river delta formation – Part 2

M. Liang et al.

Title Page

Abstract

Introduction

Conclusions

References

Tables

Figures

◀

▶

◀

▶

Back

Close

Full Screen / Esc

Printer-friendly Version

Interactive Discussion



A reduced-complexity model for river delta formation – Part 2

M. Liang et al.

Title Page

Abstract

Introduction

Conclusions

References

Tables

Figures

◀

▶

◀

▶

Back

Close

Full Screen / Esc

Printer-friendly Version

Interactive Discussion



One qualitative difference in the observed flow plan-view pattern produced by FlowRCM and Delft3D is what we call “local effects”. In the results of FlowRCM there is significant concentration of flux right upstream of the island, where flow bifurcates directly against the tip of the island (in this case, the no-flow condition at the boundary of the islands does not allow any water flux to escape the channels) (Fig. 10, dashed square region). The water surface elevation calculated by FlowRCM does not show super-elevation right at the tip of the island as in the Delft3D results; instead, there is a draw-down. We believe that the super-elevation creates a gradient that causes the flow to divert around the island much further upstream.

4.4 Test 4 results: flow through a distributary channel network

4.4.1 Test 4a: synthetic Wax Lake Delta (WLD) topography

The results show that the two models have strong agreement on the flow distribution among channels and islands, for example “hot spots” of higher flow velocity occur at the same locations (Fig. 11). Delft3D shows a more “diffused” velocity map while FlowRCM gives a more “noisy” map. The flow pattern on the islands predicted by FlowRCM seems to respond to island topography, exhibiting a converging stream in the low elevation area towards the lower center of the islands (Fig. 11). In Delft3D results, flow is more evenly distributed across each island, thus not revealing much island topographic detail (although higher resolution Delft3D modelling would, while constraints exist in its drying-flooding algorithm). The depth-averaged mode and the choice of horizontal eddy viscosity might also add to the relatively smooth outputs from Delft3D. The “local effects” in FlowRCM that we demonstrated in the previous section cause the appearance of a high velocity zone right along the tip of the islands rather than a low velocity zone caused by flow diversion starting upstream of the island as in the Delft3D results (Fig. 12).

A reduced-complexity model for river delta formation – Part 2

M. Liang et al.

Title Page

Abstract

Introduction

Conclusions

References

Tables

Figures

◀

▶

◀

▶

Back

Close

Full Screen / Esc

Printer-friendly Version

Interactive Discussion



the results in test 4a using the synthetic WLD topography, the results from Delft3D look more “diffusive” than FlowRCM. The local effects, when combined with the use of parcels, may offer a richer flow pattern in response to small changes on the floodplain. Although this observation requires further investigation, based on our results RC flow routing schemes seem to be less constrained by the complex flow boundaries caused by wet-dry partitioning in the cells than higher-fidelity models based on partial differential equations.

While the main focus of this work is the validation of the reduced-complexity flow routing scheme in the delta formation model introduced in Part 1, the validation framework we proposed can be applied to other RCMs with explicit flow routing schemes. In light of the rapid development of RCMs, we would like to make suggestions for the development of a comprehensive framework to validate RC flow routing schemes in the field of geomorphology, with an emphasis on the connection between hydrodynamic processes and morphodynamic processes. We identify the following key steps:

1. Identify key hydrodynamic processes that control the behavior of the modeled environment at the complexity level of interest.
2. Design “benchmarking” test cases (based on field data and high-fidelity numerical simulations) that reveal the model’s ability to reproduce these fundamental processes individually.
3. Perform an inter-comparison of models at different complexity levels (e.g. higher-fidelity models).
4. Identify individual or linked model rules responsible for physical and unphysical features in the model output.
5. Link the performance of the routing scheme to the morphodynamic results, especially when sediment transport in the complete morphodynamic RCM is also rule-based, it is important to identify what features in the flow solver control the resolved morphology.

6 Conclusions

In this work we have applied a series of numerical tests to validate the reduced-complexity flow routing scheme, FlowRCM, which is introduced in Part 1 (Liang et al., 2014) as the hydrodynamic component of our RC delta formation model. We selected key hydrodynamic processes essential to channel processes in deltas and designed numerical tests as “benchmarking” cases for this specific environment. We compared the output from FlowRCM with the output from a higher-fidelity hydrodynamic model, Delft3D, which is based on rigorous CFD solutions. We also used theoretical solutions to demonstrate FlowRCM’s ability to reproduce hydrodynamic details.

The results show that FlowRCM is able to reproduce most of the flow and water surface features of interest. Overall, it captures (1) the trend of water surface from upstream to downstream and from channels to floodplain, (2) flow partitioning corresponding to complex bed topography such as flow divergence and convergence around obstacles. The model shows the presence of “local effects”, a common feature of cellular routing schemes. We have also shown that the routing scheme is able to produce morphodynamic features such as mouth-bars, bifurcations and levee formation. The responsible process is an instability-feedback mechanism resulting from the coupling of the hydrodynamic component and the sediment transport rules.

This work suggests a validation framework for RCMs with explicit flow routing schemes. The key ideas include (1) designing test cases to evaluate the performance of the routing scheme in producing features related to the processes of interest; (2) identifying the effects of model rules and connecting them to model output individually; and (3) connecting the hydrodynamic to the morphodynamic performance to evaluate the flow routing scheme’s ability to model morphodynamics accurately.

Finally, we suggest that FlowRCM is appropriate for modeling environments with multi-channel networks where morphodynamic features can be produced from the estimation of channel-to-channel and channel-to-island/floodplain flow partitioning. More detailed prediction of in-channel flow patterns such as spatial distribution of high/low

A reduced-complexity model for river delta formation – Part 2

M. Liang et al.

Title Page

Abstract

Introduction

Conclusions

References

Tables

Figures



Back

Close

Full Screen / Esc

Printer-friendly Version

Interactive Discussion



velocity and surface deformation could also be achieved but it is not intended for small-scale engineering purposes.

Acknowledgements. This work was supported by the National Science Foundation Grant Nos. FESD/EAR-1135427 and GSS/BCS-1063228.

References

- Anderson, R. S. and Haff, P. K.: Simulation of eolian saltation, *Science*, 241, 820–823, 1988.
- Ashton, A., Murray, A. B., and Arnoult, O.: Formation of coastline features by large-scale instabilities induced by high-angle waves, *Nature*, 414, 296–300, 2001.
- Chow, V. T.: *Open-channel hydraulics*, in: *Open-Channel Hydraulics*, McGraw-Hill, New York, 1959.
- Coulthard, T. J., Macklin, M. G., and Kirkby, M. J.: A cellular model of Holocene upland river basin and alluvial fan evolution, *Earth Surf. Proc. Land.*, 27, 269–288, 2002.
- Duan, J. G. and Julien, P. Y.: Numerical simulation of meandering evolution, *J. Hydrol.*, 391, 34–46, 2010.
- Edmonds, D. A. and Slingerland, R. L.: Mechanics of river mouth bar formation: implications for the morphodynamics of delta distributary networks, *J. Geophys. Res.*, 112, F02034, doi:10.1029/2006JF000574, 2007.
- Edmonds, D. A. and Slingerland, R. L.: Stability of delta distributary networks and their bifurcations, *Water Resour. Res.*, 44, W09426, doi:10.1029/2008WR006992, 2008.
- Edmonds, D. A., Slingerland, R., Best, J., Parsons, D., and Smith, N.: Response of river-dominated delta channel networks to permanent changes in river discharge, *Geophys. Res. Lett.*, 37, L12404, doi:10.1029/2010GL043269, 2010.
- Edmonds, D. A., Paola, C., Hoyal, D. C. J. D., and Sheets, B. A.: Quantitative metrics that describe river deltas and their channel networks, *J. Geophys. Res.*, 116, F04022, doi:10.1029/2010JF001955, 2011.
- Ferguson, R. I., Church, M., and Weatherly, H.: Fluvial aggradation in Vedder River: testing a one-dimensional sedimentation model, *Water Resour. Res.*, 37, 3331–3347, 2001.
- Fonstad, M. A.: Cellular automata as analysis and synthesis engines at the geomorphology–ecology interface, *Geomorphology*, 77, 217–234, 2006.

A reduced-complexity model for river delta formation – Part 2

M. Liang et al.

Title Page

Abstract

Introduction

Conclusions

References

Tables

Figures

◀

▶

◀

▶

Back

Close

Full Screen / Esc

Printer-friendly Version

Interactive Discussion



A reduced-complexity model for river delta formation – Part 2

M. Liang et al.

Title Page

Abstract

Introduction

Conclusions

References

Tables

Figures

◀

▶

◀

▶

Back

Close

Full Screen / Esc

Printer-friendly Version

Interactive Discussion



- Murray, A. B. and Paola, C.: A cellular model of braided rivers, *Nature*, 371, 54–57, 1994.
- Murray, A. B. and Paola, C.: Properties of a cellular braided-stream model, *Earth Surf. Proc. Land.*, 22, 1001–1025, 1997.
- Murray, A. B. and Thieler, E. R.: A new hypothesis and exploratory model for the formation of large-scale inner-shelf sediment sorting and “rippled scour depressions”, *Cont. Shelf Res.*, 24, 295–315, 2004.
- Nicholas, A. P.: Cellular modelling in fluvial geomorphology, *Earth Surf. Proc. Land.*, 30, 645–649, 2005.
- Nicholas, A. P.: Reduced-complexity modeling of free bar morphodynamics in alluvial channels, *J. Geophys. Res.-Earth*, 115, F04021, doi:10.1029/2010JF001774, 2010.
- Nicholas, A. P.: Modelling the continuum of river channel patterns, *Earth Surf. Proc. Land.*, 38, 1187–1196, 2013.
- Nicholas, A. P., Sandbach, S. D., Ashworth, P. J., Amsler, M. L., Best, J. L., Hardy, R. J., Lane, S. N., Orfeo, O., Parsons, D. R., Reesink, A. J. H., Sambrook Smith, G. H., and Szupiany, R. N.: Modelling hydrodynamics in the Rio Paraná, Argentina: an evaluation and inter-comparison of reduced-complexity and physics based models applied to a large sand-bed river, *Geomorphology*, 169–170, 192–211, 2012.
- Overeem, I., Syvitski, J. P. M., and Hutton, E. W. H.: Three-dimensional numerical modeling of deltas, in: *River Deltas: Concepts, Models and Examples*, edited by: Bhattacharya, J. P. and Giosan, L., *SEPM Spec. Publ.*, 83, SEPM, Tulsa, 13–30, 2005.
- Paola, C., Twilley, R. R., Edmonds, D. A., Kim, W., Mohrig, D., Parker, G., Viparelli, E., and Voller, V. R.: Natural processes in delta restoration: application to the Mississippi Delta, *Ann. Rev. Mar. Sci.*, 3, 67–91, 2011.
- Passalacqua, P., Lanzoni, S., Paola, C., and Rinaldo, A.: Geomorphic signatures of deltaic processes and vegetation: the Ganges-Brahmaputra-Jamuna case study, *J. Geophys. Res.-Earth*, 118, 1838–1849, 2013.
- Roberts, H., Adams, R., and Cunningham, R.: Evolution of sand-dominant subaerial phase, Atchafalaya Delta, Louisiana, *AAPG Bull.*, 64, 264–279, 1980.
- Shaw, J. B., Mohrig, D., and Whitman, S. K.: The morphology and evolution of channels on the Wax Lake Delta, Louisiana, USA, *J. Geophys. Res.-Earth*, 118, 1–23, 2013.
- Siviglia, A., Stecca, G., Vanzo, D., Zolezzi, G., Toro, E. F., and Tubino, M.: Numerical modelling of two-dimensional morphodynamics with applications to river bars and bifurcations, *Adv. Water Resour.*, 52, 243–260, 2013.

A reduced-complexity model for river delta formation – Part 2

M. Liang et al.

Title Page

Abstract

Introduction

Conclusions

References

Tables

Figures

⏪

⏩

◀

▶

Back

Close

Full Screen / Esc

Printer-friendly Version

Interactive Discussion



- Sun, T., Paola, C., Parker, G., and Meakin, P.: Fluvial fan deltas: linking channel processes with large-scale morphodynamics, *Water Resour. Res.*, **38**, 26-21–26-10, 2002.
- Thomas, R. and Nicholas, A.: Simulation of braided river flow using a new cellular routing scheme, *Geomorphology*, **43**, 179–195, 2002.
- 5 Tucker, G. E. and Bras, R. L.: Hillslope processes, drainage density, and landscape morphology, *Water Resour. Res.*, **34**, 2751–2764, 1998.
- USACE – US Army Corps of Engineers: Atchafalaya River hydrographic survey, 1998–1999: Old River to Atchafalaya Bay including main channel and distributaries, The District, New Orleans, LA, 1999.
- 10 Wellner, R., Beaubouef, R., Van Wagoner, J., Roberts, H., and Sun, T.: Jet-plume depositional bodies – the primary building blocks of Wax Lake delta, *Gulf Coast Association of Geological Society Transactions*, Vol. 55, 867–909, 2005.
- Werner, B.: Eolian dunes: computer simulations and attractor interpretation, *Geology*, **23**, 1107–1110, 1995.
- 15 Willgoose, G.: A statistic for testing the elevation characteristics of landscape simulation models, *J. Geophys. Res.-Sol. Ea.*, **99**, 13987–13996, 1994.
- Wolinsky, M. A., Edmonds, D. A., Martin, J., and Paola, C.: Delta allometry: growth laws for river deltas, *Geophys. Res. Lett.*, **37**, L21403, doi:10.1029/2010GL044592, 2010.

A reduced-complexity model for river delta formation – Part 2

M. Liang et al.

Table 1. Discharge asymmetry and upstream surface elevation results from FlowRCM and Delft3D for all single bifurcation runs.

Run #	Discharge Asymmetry (%)			Upstream Surface Elevation (m)		
	FlowRCM	Delft3D	difference	FlowRCM	Delft3D	difference
A1	0.16 %	0.00 %	+0.16 %	0.3226	0.2067	+0.1159
A2	20.82 %	24.04 %	−3.23 %	0.3160	0.2048	+0.1112
A3	41.04 %	47.69 %	−6.65 %	0.3156	0.2016	+0.1140
B1	0.16 %	0.00 %	+0.16 %	0.3226	0.2067	+0.1159
B2	21.59 %	21.17 %	+0.42 %	0.3230	0.2068	+0.1162
B3	40.76 %	42.78 %	−2.02 %	0.3301	0.2075	+0.1226
C1	0.21 %	0.01 %	+0.19 %	0.1472	0.1091	+0.0381
C2	28.22 %	27.84 %	+0.37 %	0.1417	0.1057	+0.0360
C3	51.49 %	52.66 %	−1.17 %	0.1286	0.0963	+0.0323

Title Page

Abstract

Introduction

Conclusions

References

Tables

Figures

◀

▶

◀

▶

Back

Close

Full Screen / Esc

Printer-friendly Version

Interactive Discussion



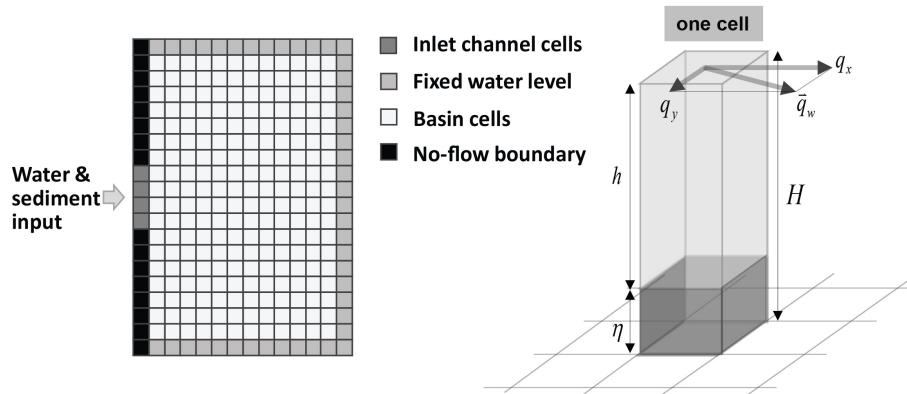


Figure 1. Basic setup of the model. The calculation domain is represented by a lattice of square cells (shown as a cartoon on the left). Primary quantities associated with each cell include flow depth, water surface elevation, bed elevation and flow unit discharge vector.

A reduced-complexity model for river delta formation – Part 2

M. Liang et al.

Title Page

Abstract

Introduction

Conclusions

References

Tables

Figures



Back

Close

Full Screen / Esc

Printer-friendly Version

Interactive Discussion



A reduced-complexity model for river delta formation – Part 2

M. Liang et al.

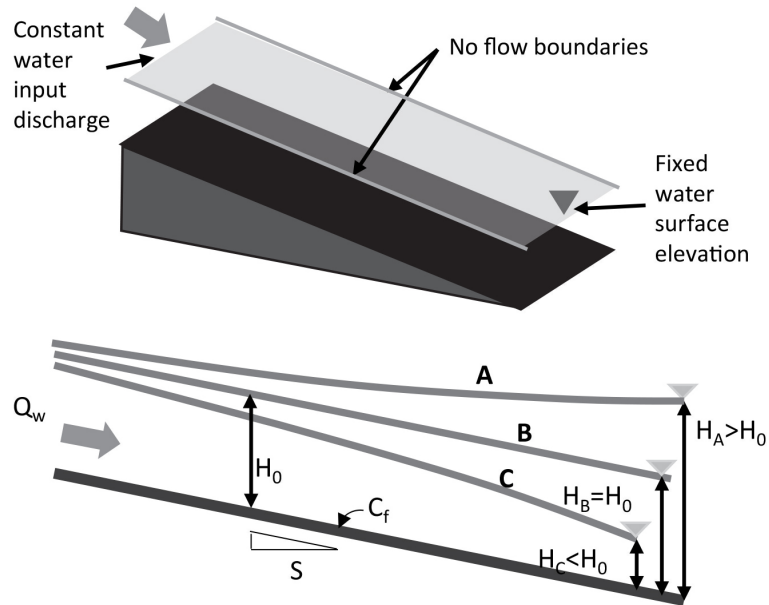


Figure 2. The setup of the straight channel test. The channel has a rectangular cross-section. The bed has a constant slope and a constant friction coefficient. A constant discharge is fed into the upstream inlet. The downstream outlet has a fixed water surface elevation as boundary condition. Three backwater profiles are shown in the bottom cartoon where downstream water surface elevation is above, equal to, or below that of normal flow.

Title Page

Abstract

Introduction

Conclusions

References

Tables

Figures

◀

▶

◀

▶

Back

Close

Full Screen / Esc

Printer-friendly Version

Interactive Discussion



A reduced-complexity model for river delta formation – Part 2

M. Liang et al.

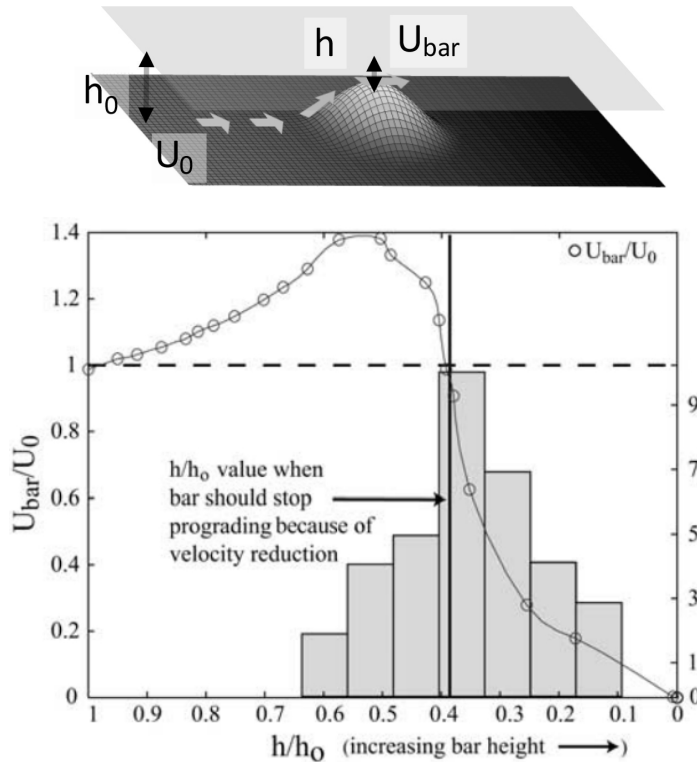


Figure 3. Setup of the bump test (flow around a mouth bar). A smooth Gaussian-shape bump is placed in a straight channel where we observe two scenarios of flow interacting with the bump topography: (i) acceleration over the bump or, (ii) deceleration over the bump and diversion around the bump. The lower plot is taken from Edmonds and Slingerland (2007), where they show the transition between the two scenarios as channel mouth bar grows in height.

A reduced-complexity model for river delta formation – Part 2

M. Liang et al.

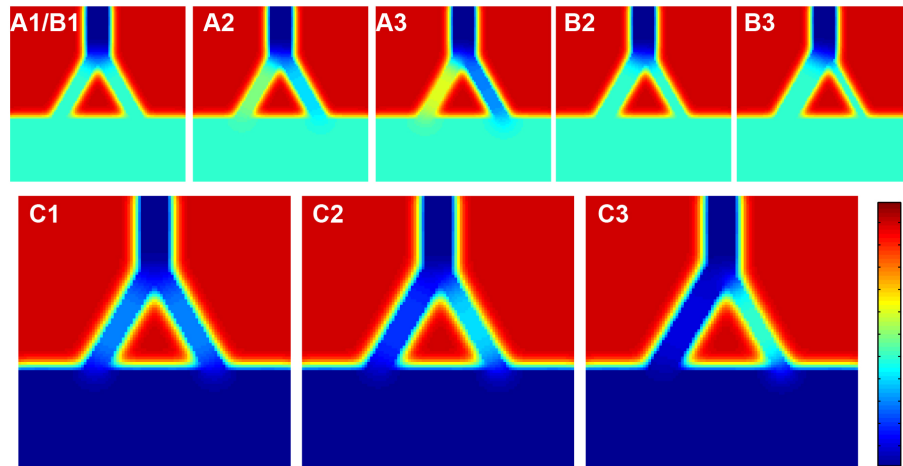


Figure 4. Channel geometries for the single bifurcation test. Group A (A1, A2 and A3) and group B (B1, B2 and B3) have smaller domain and input discharge. Within group A we vary the ratio of depth between the two downstream branches while keeping width constant. Within group B we vary the ratio of width between the two downstream branches while keeping the depth constant. Within group C (C1, C2 and C3) we vary width and depth at the same proportion while keeping the summation of cross-sectional area constant.

Title Page

Abstract

Introduction

Conclusions

References

Tables

Figures

◀

▶

◀

▶

Back

Close

Full Screen / Esc

Printer-friendly Version

Interactive Discussion



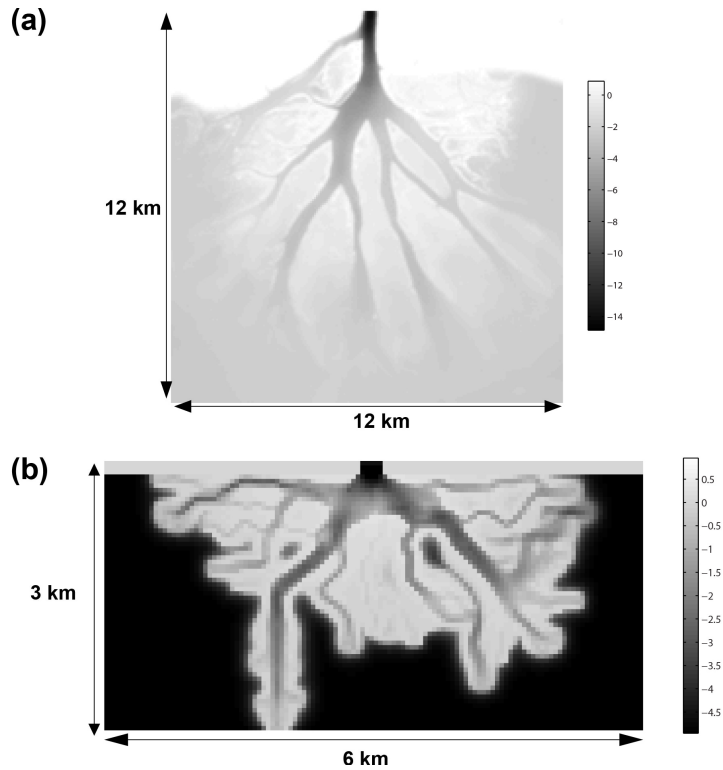


Figure 5. Topography for the tests on flow through a distributary channel network. **(a)** A synthetic topography constructed for Wax Lake Delta; **(b)** a DeltaRCM generated delta topography.

A reduced-complexity model for river delta formation – Part 2

M. Liang et al.

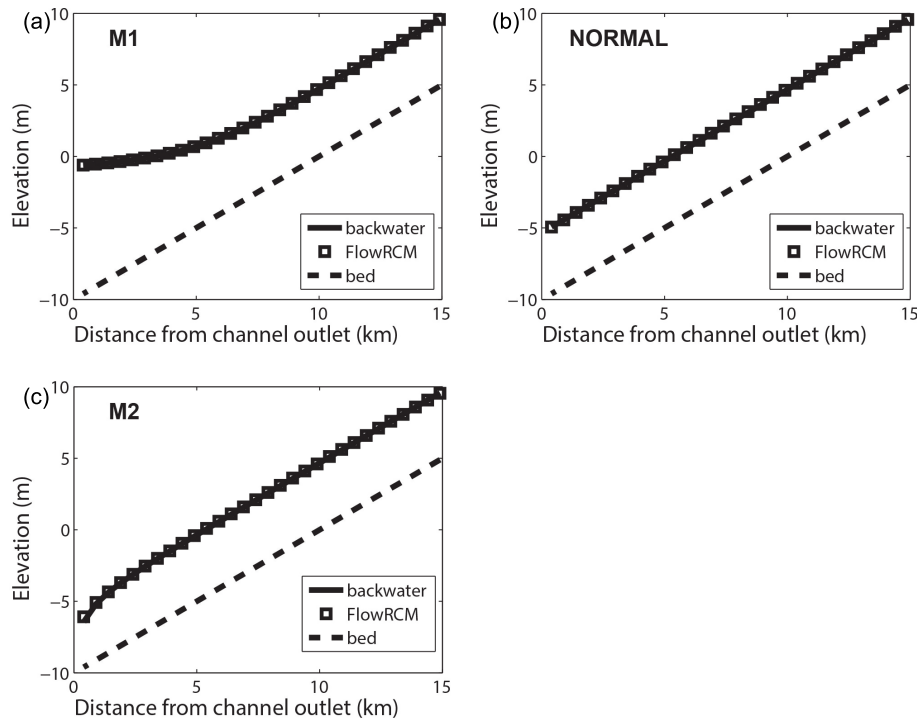


Figure 6. Results from the straight channel test. Cross-stream averaged water surface profile calculated by FlowRCM is compared to the numerical solution of backwater equation. **(a)** Downstream water surface elevation is fixed at higher than that of normal flow (M1 curve). **(b)** Downstream water surface elevation is fixed at that of normal flow. **(c)** Downstream water surface elevation is fixed at lower than that of normal flow (M2 curve).

Title Page

Abstract

Introduction

Conclusions

References

Tables

Figures

◀

▶

◀

▶

Back

Close

Full Screen / Esc

Printer-friendly Version

Interactive Discussion



A reduced-complexity model for river delta formation – Part 2

M. Liang et al.

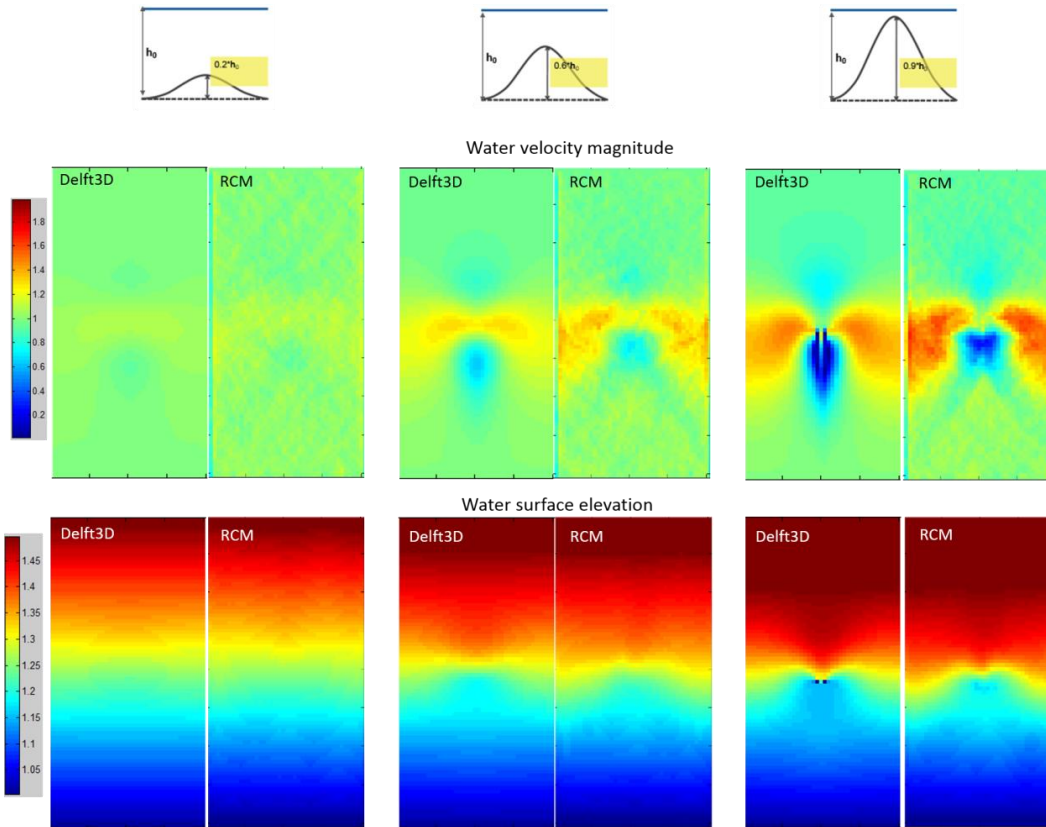


Figure 7. Water velocity magnitude (normalized by the upstream velocity magnitude) and water surface elevation contour plots (bump height at 20, 60 and 90 % flow depth). Flow direction is from top to bottom. Notice the deformation of water surface and the development of low velocity region in front of and behind the bump.

Title Page

Abstract

Introduction

Conclusions

References

Tables

Figures



Back

Close

Full Screen / Esc

Printer-friendly Version

Interactive Discussion



A reduced-complexity model for river delta formation – Part 2

M. Liang et al.

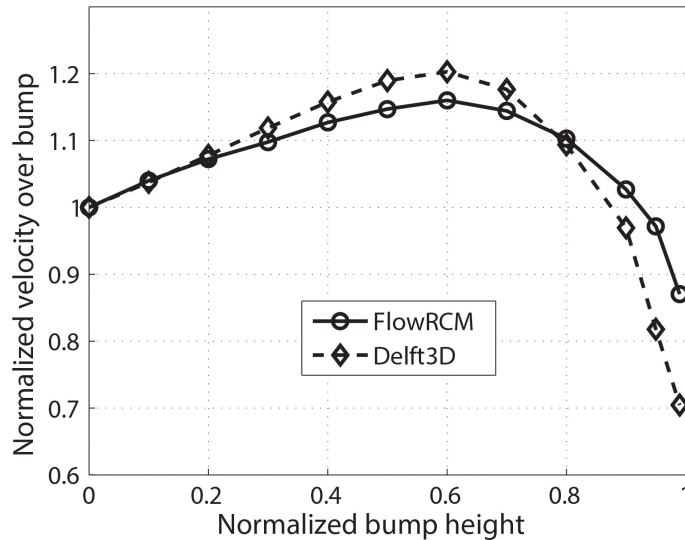


Figure 8. Both FlowRCM and Delft3D predict a rising then falling normalized flow velocity (measured at the top of the bump) as normalized bump height goes to 1. FlowRCM also captures the turning point where rising changes to falling ($\sim 60\%$ flow depth). Flow velocity is normalized by the upstream velocity magnitude, and bump height is normalized by water depth.

[Title Page](#)[Abstract](#)[Introduction](#)[Conclusions](#)[References](#)[Tables](#)[Figures](#)[◀](#)[▶](#)[◀](#)[▶](#)[Back](#)[Close](#)[Full Screen / Esc](#)[Printer-friendly Version](#)[Interactive Discussion](#)

A reduced-complexity model for river delta formation – Part 2

M. Liang et al.

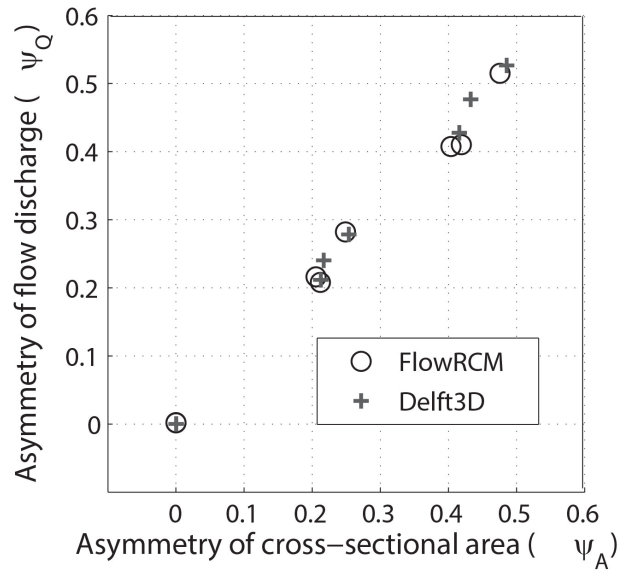


Figure 9. The discharge asymmetry and the cross-sectional areas asymmetry of the two bifurcation branches compare well between FlowRCM and Delft3D simulations. Overall the asymmetry of discharge is proportional to the asymmetry of cross-sectional area.

Title Page

Abstract

Introduction

Conclusions

References

Tables

Figures

◀

▶

◀

▶

Back

Close

Full Screen / Esc

Printer-friendly Version

Interactive Discussion



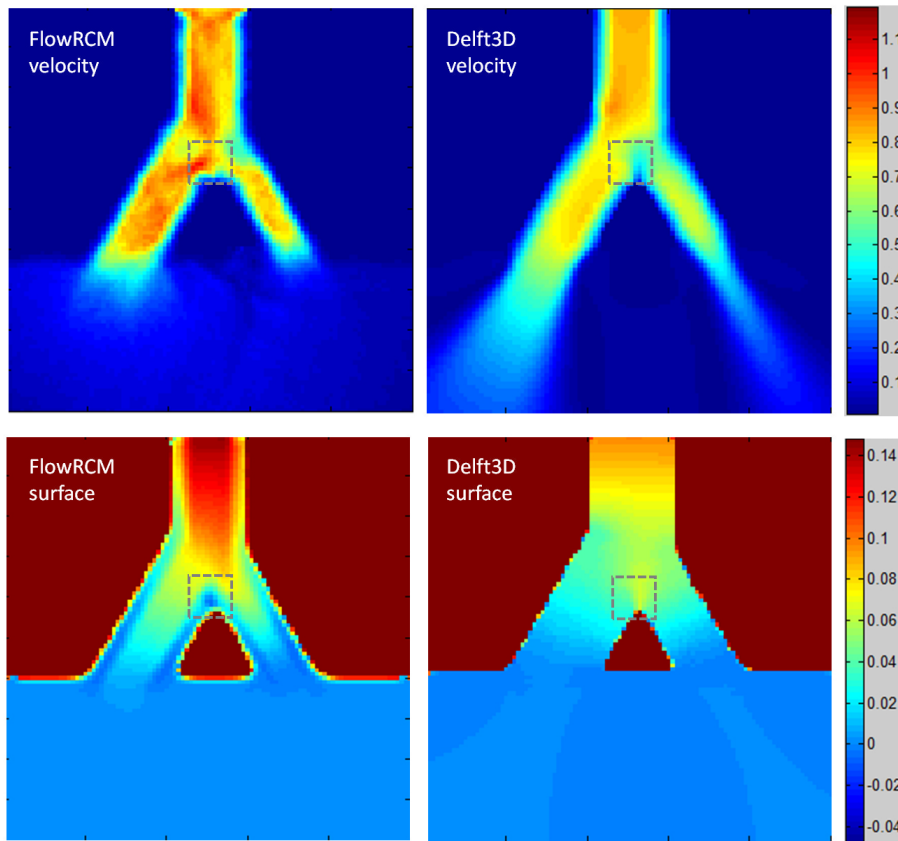


Figure 10. Velocity and water surface contour plots from Run C3. In dashed square region is the qualitative difference between FlowRCM and Delft3D results: upstream of the front tip of the island, while Delft3D exhibits a low velocity zone with a high water surface elevation, FlowRCM exhibits a high velocity and a low water surface elevation.

A reduced-complexity model for river delta formation – Part 2

M. Liang et al.

Title Page

Abstract

Introduction

Conclusions

References

Tables

Figures

◀

▶

◀

▶

Back

Close

Full Screen / Esc

Printer-friendly Version

Interactive Discussion



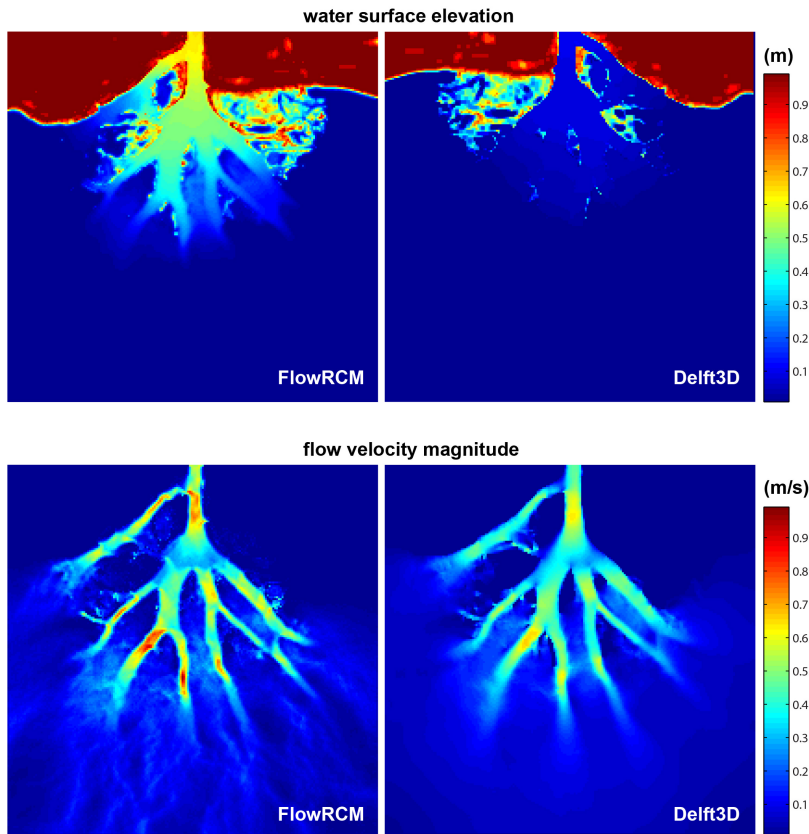


Figure 11. Hydrodynamic test calculating flow patterns over the synthetic bathymetry of Wax Lake Delta (WLD) in Louisiana. **(a)** Water surface profiles from the two models have similar distribution but FlowRCM predicts a significantly higher gradient. **(b)** Velocity contour maps from model results; FlowRCM and Delft3D give similar flow distributions, and predict “hot zones” where water velocity is significantly higher in channels at the same locations.

A reduced-complexity model for river delta formation – Part 2

M. Liang et al.

Title Page

Abstract Introduction

Conclusions References

Tables Figures

◀ ▶

◀ ▶

Back Close

Full Screen / Esc

Printer-friendly Version

Interactive Discussion



A reduced-complexity model for river delta formation – Part 2

M. Liang et al.

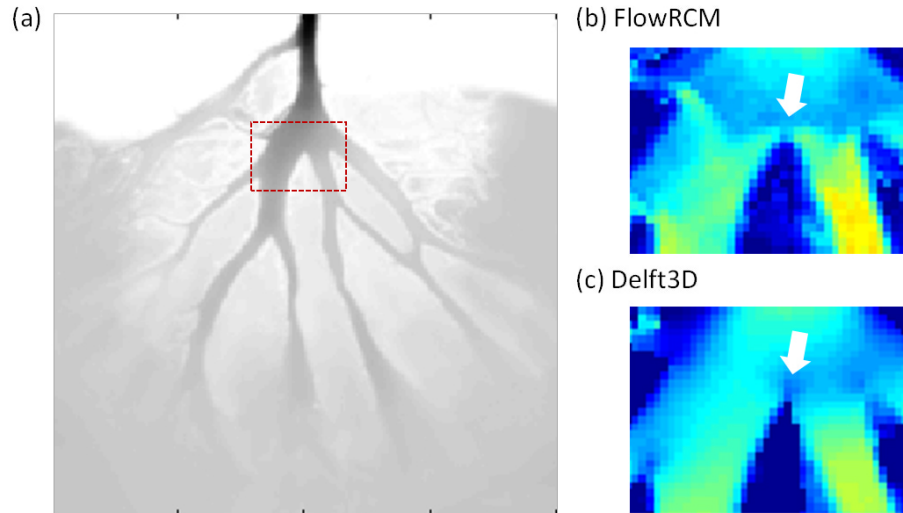


Figure 12. (a) red dashed square marks one of the regions where FlowRCM display strong local effects (b) detailed view from both models' results demonstrate the “local effects” created by FlowRCM, which are not present in the Delft3D simulation.

Title Page

Abstract

Introduction

Conclusions

References

Tables

Figures

◀

▶

◀

▶

Back

Close

Full Screen / Esc

Printer-friendly Version

Interactive Discussion



A reduced-complexity model for river delta formation – Part 2

M. Liang et al.

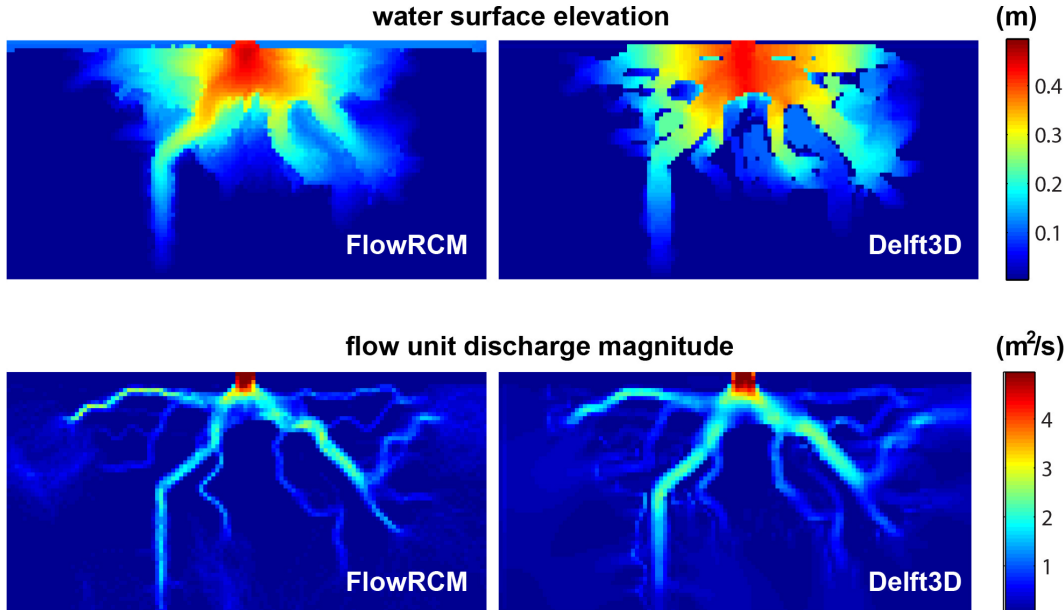


Figure 13. Flow test results using DeltaRCM generated delta topography. The water surface elevation and unit discharge from the outputs of the RCM model are compared to the results from running Delft3D hydrodynamic module with the same topography and input conditions. The results show that: (1) both models give similar discharge distribution throughout the topography; (2) both models give similar water surface profile: same magnitude, although RCM has a more consistent surface profile and more pronounced gradient across the channel into the floodplains.

Title Page

Abstract Introduction

Conclusions References

Tables Figures

◀ ▶

◀ ▶

Back Close

Full Screen / Esc

Printer-friendly Version

Interactive Discussion



A reduced-complexity model for river delta formation – Part 2

M. Liang et al.

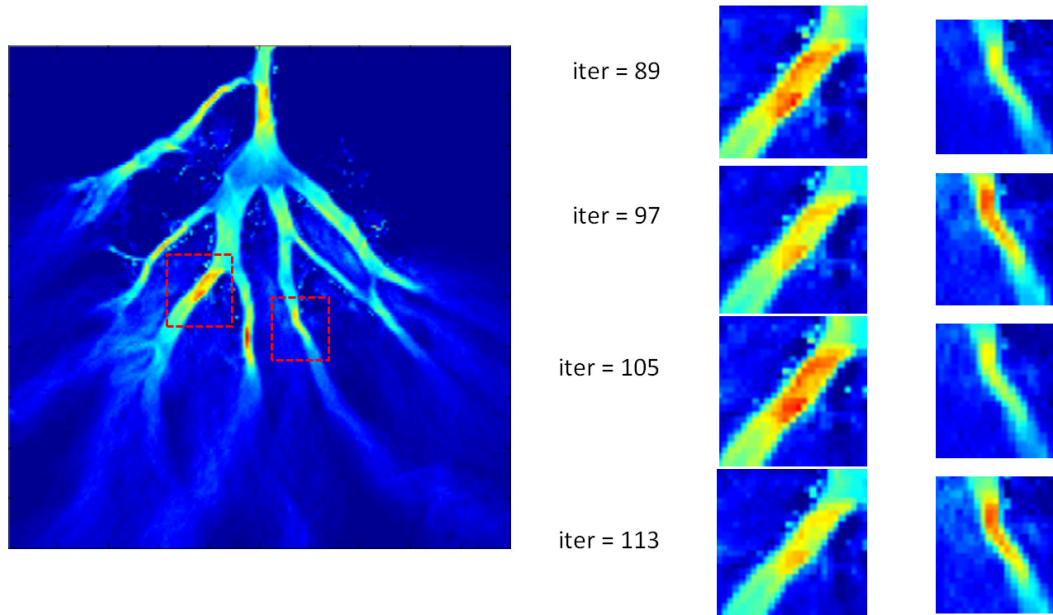


Figure 14. The dynamic balance between water surface gradient and flux distribution. On the left the dashed square shows the region of enlarged areas. On the right it shows the oscillations of flow velocity between iterations in the enlarged areas.

Title Page

Abstract

Introduction

Conclusions

References

Tables

Figures

◀

▶

◀

▶

Back

Close

Full Screen / Esc

Printer-friendly Version

Interactive Discussion



A reduced-complexity model for river delta formation – Part 2

M. Liang et al.

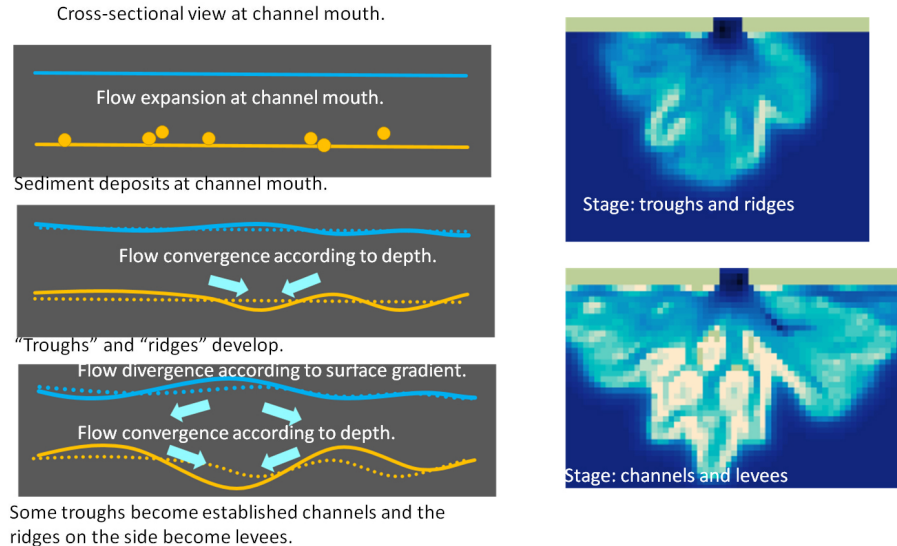


Figure 15. Illustration of the mechanics of bifurcation formation in the DeltaRCM. (i) flow expands and sediment deposits with reduced flow velocity, which creates a wide lunate bar with noisy surface; (ii) the irregular topography of the bar forms “ridges” and “troughs” where troughs attract more water flux than ridges; (iii) the enhanced flow rate in troughs prevents sediment from settling while ridges continue to experience deposition; (iv) the process reaches equilibrium by the feedback mechanism between water surface elevation and water flux. The few paths established from the troughs outcompete the others.

Title Page	
Abstract	Introduction
Conclusions	References
Tables	Figures
◀	▶
◀	▶
Back	Close
Full Screen / Esc	
Printer-friendly Version	
Interactive Discussion	

